NANO LETTERS

2007
Vol. 7, No. 8
2428−2434

Dynamics of Carbon Nanotube Growth from Fullerenes

Rudolf Pfeiffer,*,† Matthias Holzweber,† Herwig Peterlik,† Hans Kuzmany,† Zheng Liu,‡ Kazu Suenaga,‡ and Hiromichi Kataura‡

Fakultät für Physik, Universität Wien, Strudlhofgasse 4, 1090 Wien, Austria, and AIST, Tsukuba, Japan

Received May 11, 2007; Revised Manuscript Received June 6, 2007

ABSTRACT

The growth of double-walled carbon nanotubes from peapods was studied. The transformation was monitored by the decrease of fullerene Raman lines, the growth of inner tube Raman lines, and the development of X-ray diffraction patterns. A visual check of the growth process by HRTEM provided additional information. From the difference in time constants for the bleaching of fullerene Raman lines and for the growth of nanotube Raman lines, the existence of an intermediate phase was concluded that was eventually observed in X-ray diffraction and HRTEM. Time constants for the growth of large diameter inner tubes were up to a factor two larger than for small diameter inner tubes. The results fully support the fullerene coalescence growth model triggered by Stone–Wales transformations.

Double-wall carbon nanotubes (DWCNTs) can be grown either directly, e.g., in a CVD process,[1] or by annealing single-wall carbon nanotubes (SWCNTs) encapsulating carbon-rich precursor molecules. The most prominent example for the latter are DWCNTs grown from (C_{60}) peapods, i.e., SWCNTs filled with (C_{60}) fullerenes.[2] The particular advantage of DWCNTs produced from filled SWCNTs is the growth of the inner tubes in a highly shielded environment,[3] and, in the case of peapods, without any additional catalyst. This opens the possibility for a detailed study of carbon nanotube growth in a clean room of about 1.4 nm width. Additionally, by employing ^{13}C enriched precursors, one can selectively isotope-label the inner tubes. In this way, NMR studies on nanotubes without other interfering carbon phases became possible.[4,5]

Several factors influence the growth rate, the volume fraction, and the diameter distribution of the inner tubes: (i) the diameter distribution of the outer SWCNTs,[6] (ii) the diameter range, which can be filled with the precursor, (iii) the precursor itself, (iv) the filling ratio, and (v) annealing time and temperature. Here, we report a detailed Raman scattering, X-ray diffraction (XRD), and high-resolution transmission electron microscopy (HRTEM) analysis for the growth process of the inner tubes of C_{60}@SWCNTs based DWCNTs. These methods provide complementary structural information: Raman is sensitive to the vibrational modes of specific resonance-selected SWCNTs and fullerenes, XRD gives information on the periodic arrangement of the SWCNTs and the fullerenes (or other species) within the tubes, and HRTEM allows visualization of the individual tubes and materials inside.

One of the significant features in the Raman spectra of SWCNTs is the response from the radial breathing mode (RBM), which is usually observed between 100 and 250 cm^{-1}. The frequency of this mode is roughly proportional to the inverse tube diameter and is often used to determine the diameter distribution in macroscopic samples.[7] For a unique assignment of an RBM peak to a specific tube chirality (m,n), the optical transition energies of the tubes have also to be considered. Several groups recorded Raman maps—i.e., contour plots of the RBM intensity vs frequency and excitation energy—of individual SWCNTs dispersed in SDS.[8,9] A similar Raman map of buckypaper DWCNTs was reported recently from our group.[10] In this map, a specific inner tube gives rise to a whole cluster of peaks. The clusters originate from the fact that one and the same inner tube type can grow in several different outer tube types. The inner tube−outer tube interaction depends on the diameter difference of the two concentric shells. The larger the interaction, the further the inner tube RBM shifts to higher frequencies.[11]

XRD gives information on the periodic arrangement of SWCNTs within macroscopic samples. From the position and intensity of the peaks in the XRD pattern, one obtains the arrangement of bundled tubes in a 2D hexagonal lattice, the mean tube diameter, and the van der Waals distance between the tubes.[7] Peapods feature additional peaks due to the 1D chain formed by the encaged fullerenes. The intensity of the peaks is modulated by the form factor, which is

* Corresponding author. E-mail: rudolf.pfeiffer@univie.ac.at. Telephone: +43 1 4277 51378.
† Universität Wien.
‡ AIST.

10.1021/nl071107o CCC: $37.00
Published on Web 07/03/2007

different for empty SWCNTs, SWCNTs filled with fullerenes, and DWCNTs. This enables the determination of the amount of filling.[12]

The most direct information on peapods and DWCNTs comes from HRTEM images. From these images, the distances between fullerenes inside SWCNTs and the wall-to-wall distance of DWCNTs can be determined and, as it will be shown below, transient phases can be seen.

The growth of the inner tubes from fullerenes was studied previously by analyzing the inner tubes RBM Raman response after various heating steps.[13,14] However, no attention was paid to the fine structure of the inner tube RBM clusters. Also, the decay of the fullerene precursors was not studied simultaneously, even though this is a crucial indicator for the transformation process. Similarly, to the best of our knowledge, XRD studies were reported so far only for empty SWCNTs, C_{60} peapods, and completely transformed DWCNTs.[15] A study for the transient state is missing although it will reveal details of the growth mechanism. As a consequence of the completely different starting conditions (metal catalyst triggered growth on the one side and preformed cage structures on the other side), the growth mechanism in the peapod systems can be expected to be strongly different compared to conventional growth.

In this Letter, we focus on the decay of the encapsulated C_{60} fullerenes and their transformation into DWCNTs. After the expulsion of some C_{60} molecules from the tubes in the first minutes, the fullerene Raman signal disappears almost a factor five faster than the XRD signal from the 1D chain formed from the fullerenes within the SWCNTs. From this, the existence of an intermediate solid phase is concluded. The growth dynamics of the inner tubes depends primarily on their diameter, where the growth of the thin inner tubes coincides well with the 1D chain decay. The thicker inner tubes grow a factor two more slowly. In the coalescence model, a large number of Stone−Wales transformations required to reach the final tube diameter can be made responsible for the time delay observed for the larger diameter tubes. Additionally, at least for the thinner inner tubes, the early growth stages depend on the diameter difference between inner and outer tubes.

The starting material for our peapods were highly purified SWCNTs (mean diameter 1.39 nm, $\sigma = 0.1$ nm) prepared by laser ablation. These tubes were filled with C_{60} fullerenes as described previously.[16] For each transformation experiment, a new piece of the so-prepared peapod buckypaper was used. The Raman spectra were recorded at 80 K in a 180° backscattering geometry with a Dilor xy triple monochromator spectrometer in normal resolution or, if required, in high resolution. Because Raman intensities by themselves are not a good measure for the tube growth due to cross section problems, only intensities relative to final intensities are considered. These values are not only cross section independent but also independent from the abundance and provide direct insight into the growth dynamics. Structural characterization by X-ray diffraction was performed at room temperature with Cu K_α radiation. Raman spectra, XRD patterns, and HRTEM images were recorded on the same sample after each transformation step.

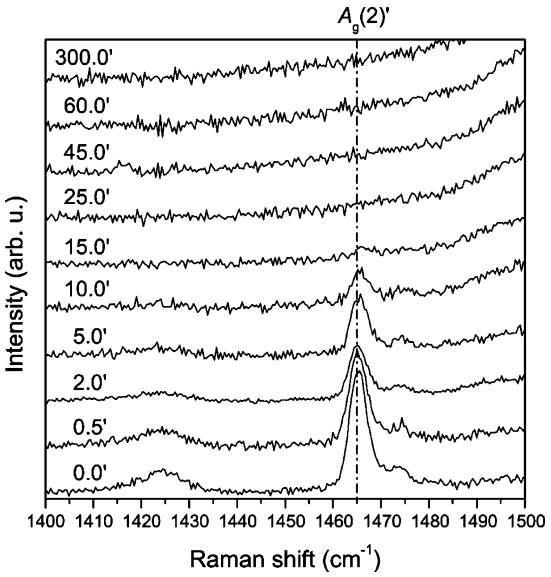

Figure 1. The 488 nm Raman spectra of the C_{60} tangential molecular vibrations measured at 80 K in normal resolution mode. Annealing times at 1250 °C are given in minutes. All spectra were normalized to the G^+ mode of the semiconducting outer SWCNTs at 1594 cm^{-1}.

The strongest and most prominent Raman mode of C_{60} is the so-called $A_g(2)$ or pentagonal-pinch mode at 1468 cm^{-1}. When the fullerenes are encapsulated into SWCNTs with diameters $\leq$1.4 nm (as is the case here), the $A_g(2)$ mode splits into a strong $A_g(2)'$ component at 1465 cm^{-1} and a weak $A_g(2)''$ component at 1473 cm^{-1}.[17] Both components are best observed for 488 nm excitation. To study the decay of the encaged C_{60} fullerenes with transformation, we recorded the tangential mode region of peapods heat treated for various time intervals (see Figure 1). The spectrum of the untreated peapods shows a strong $A_g(2)'$ mode. After an annealing time of only 0.5 min, its intensity is already reduced. For longer heating times, the intensity continues to decrease until after 15.0 min exposure it can hardly be observed any more. A similar behavior is found for the weaker $H_g(7)$ (around 1425 cm^{-1}) and $A_g(2)''$ modes. The increasing background above 1480 cm^{-1} is due to the G-modes of the growing inner tubes. Fitting an exponential decay through the intensities of the C_{60} modes as a function of transformation time yields a half-lifetime of the fullerenes of 2.9(5) min. No shift or broadening of the $A_g(2)'$ mode, and no new lines from possible reaction products other than inner tubes could be observed.

In the XRD patterns of peapods (see Figure 2, spectrum 0.0′), the (10), (11), (21), (22), and (31) peaks reflect the arrangement of the bundled SWCNTs in a hexagonal 2D lattice. The intrinsically asymmetric (001) peak at $q \approx 6.6$ nm^{-1} (and also the (002) peak) originates from the 1D chains of encapsulated fullerenes. Figure 2a shows the development of the peapod XRD patterns after thermal treatment at 1250 °C for different exposure times. All patterns were normalized to the amplitude of the graphite peak. Figure 2b is a simulation of the experimental results using

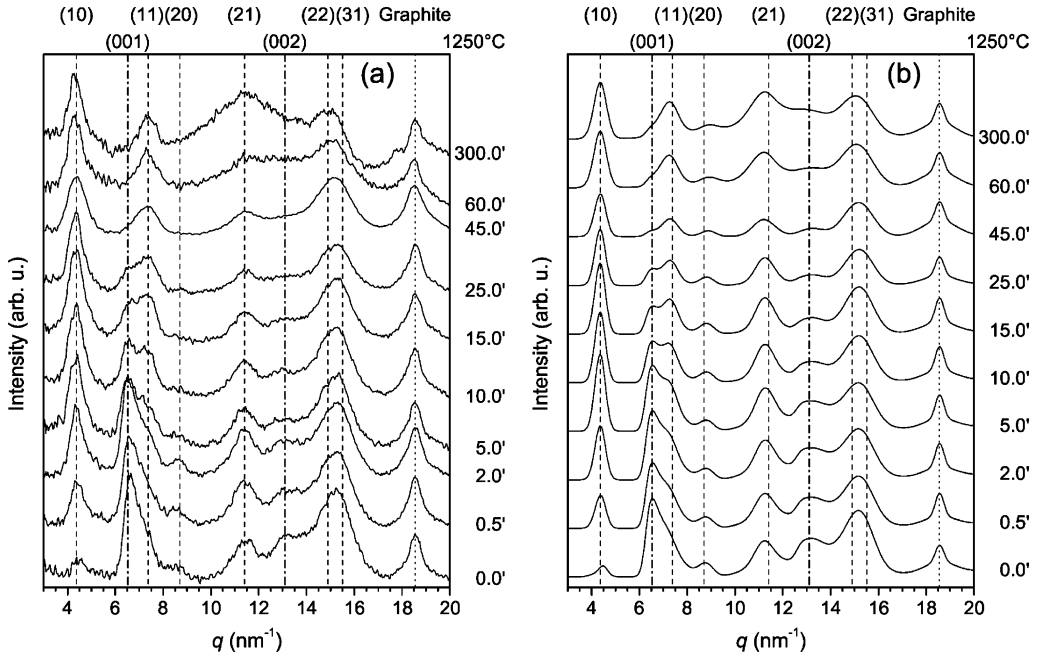

Figure 2. (a) Room-temperature XRD patterns of C_{60} peapods transformed to DWCNTs at 1250 °C for various transformation times in min and (b) the corresponding simulated patterns as described in the text. All patterns were normalized to the amplitude of the graphite peak. Bundle peaks are indicated by dashed lines, 1D chain peaks are indicated by thick dash−dotted lines, and the graphite peak is indicated by a dotted line. The positions of the vertical lines are identical in (a) and (b).

the model of Cambedouzou et al.[18] This model takes empty tubes, filled tubes, and, in the later stage of transformation, also DWCNTs into account. In contrast to ref 18, we used Gaussian distributions with increasing half-width (for distortion correction) for the lattice term for simplicity. This is justified by the high cristallinity of the tubes, as demonstrated from the large number of observed peaks. The calculated patterns nearly perfectly match the experimental data. Two main features are visible: the increase of the first bundle peak (10) at $q \approx 4.4$ nm^{-1} and the decrease of the (001) chain peak with increasing time of thermal treatment. The (10) peak is small but not negligible at the beginning. Immediately after starting the transformation, the intensity of this peak increases suddenly to more than 50% of its final value. The intensity decrease of the (001) chain peak was fitted with an exponential decay resulting in a half-lifetime of 14(2) min, which is almost five times the value for the decay of the pentagonal pinch mode of the fullerenes. This result strongly indicates that the periodicity of an intermediate reaction product remains the same as the periodicity of the C_{60} molecules for a much longer time than the pristine C_{60} shape.

The growth of the inner tubes was in detail monitored by the relative intensity increase of the inner tube RBM clusters. Figure 3 depicts as an example the growth of the clusters of tube families $2m + n = 19$ (between 280 and 320 cm^{-1}) and $2m + n = 16$ (around 365 cm^{-1}). For the used laser, the largest contributions originate respectively from the (8,3) tube with a diameter of about 0.77 nm and from the (7,2) tube with a diameter of about 0.64 nm, both resonating with E_{22}^{S}. The intensities were normalized to the outer tube RBMs around 180 cm^{-1}, which—for an excitation energy of 1.83 eV and the diameter distribution in our sample—originate only from metallic species resonating with E_{11}^{m}. A close inspection of the spectra reveals that the first weak RBM peaks of the (7,2) and (8,3) inner tubes can be observed already after 2 and 5 min, respectively. After 25 min, there is almost no further change in the (7,2) intensity, but the (8,3) intensity continues to increase by a factor of about 3 until after the 60 min treatment, where saturation is reached.

To evaluate the growth dynamics in more detail, we plot the RBM intensities of these two tubes as a function of transformation time in Figure 4. To simplify the plot, we show only the growth of the whole cluster and not that of each individual peak. From the figure, the growth of the (7,2) tube starts much earlier than the growth of the (8,3) tube and it also saturates much earlier.

The growth behavior was fitted with a Gompertz-like function, namely

$$I = A[e^{B(1-e^{-Ct})} - 1]$$

where A, B, and C are phenomenological constants. The maximum intensity ($t \rightarrow \infty$) is $A(e^B - 1)$. Half of this maximum is reached at the time $T_{1/2} = -1/C \ln[1 + 1/B \ln 2/(e^B + 1)]$. This growth half-time of the (7,2) tube is about 16 min, which is in very good agreement with the half-lifetime of the 1D chain decay obtained from the XRD measurements. The (8,3) inner tubes grow slower and reach half of their maximum volume fraction only after about 38 min. The maximum growth rate is reached at the time $t = (\ln B)/C$, which is about 12 min for the (7,2) and 31 min for the (8,3) tube. Hence most of the (8,3) growth occurs after half of the starting fullerene material was lost according

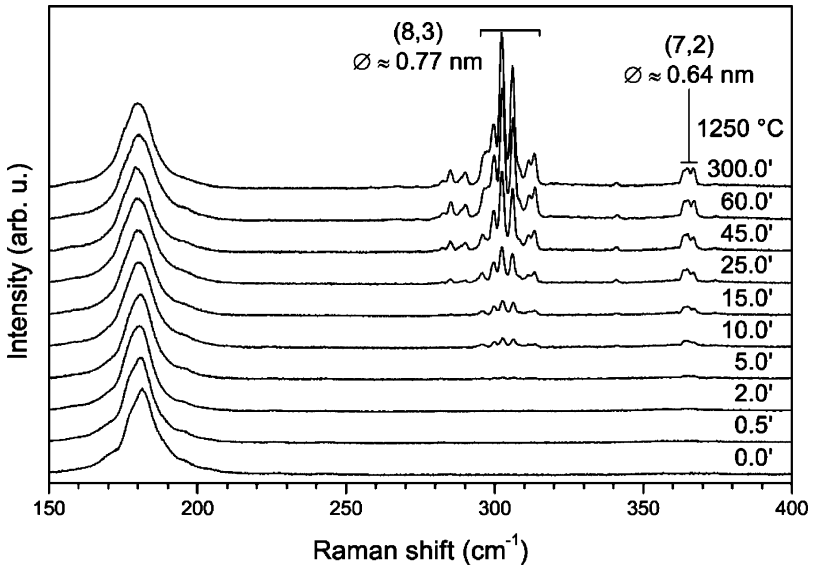

Figure 3. The 676 nm Raman spectra of the outer and inner tubes RBM region measured at 80 K in normal resolution mode. Annealing times at 1250 °C are given in min. All spectra were normalized to the outer tube RBMs around 180 cm^{-1}. Between 280 and 320 cm^{-1}, one can see the RBMs of mainly the (8,3) inner tubes, and around 365 cm^{-1}, one can observe the cluster of the (7,2) inner tubes.

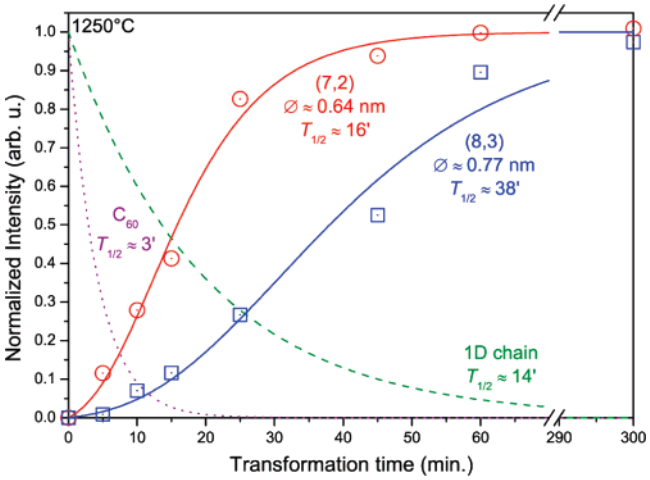

Figure 4. RBM intensity of the (7,2) and (8,3) inner tubes as a function of transformation time. The intensities for each tube were normalized to the corresponding maxima of the fit curves. The dotted and dashed lines show the exponential decays of the C_{60} Raman signal and the XRD 1D chain peak, respectively. $T_{1/2}$ are the corresponding halftimes. Note the break in the time axis between 70 and 290 min.

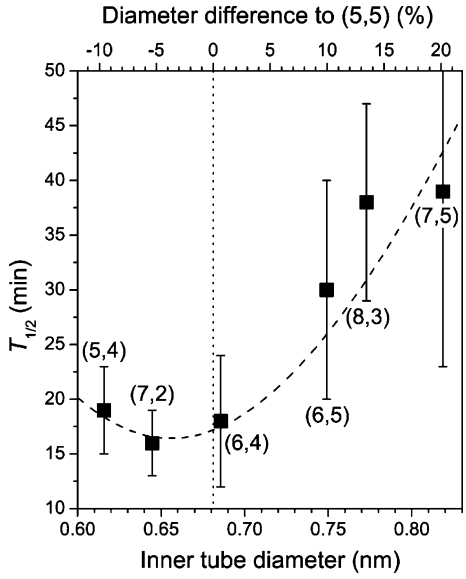

Figure 5. Growth time $T_{1/2}$ as a function of inner tube diameter. The dotted line marks the diameter of the (5,5) tube. The dashed curve is a guide for the eye. The tube diameters D were calculated with eq 2 in ref 19.

to the XRD analysis. Even more interesting, the growth of both tube types continues long after the fullerene molecules are either destroyed or expelled from the tubes according to the Raman analysis.

Using different lasers for the Raman excitation, the growth dynamics of several inner tubes was recorded. Figure 5 compares the $T_{1/2}$ times of all evaluated tubes. According to the coalescence model, the (5,5) tube—having the same diameter as C_{60}—should grow fastest. However, because the resonance for this tube is in the UV, we could not detect it. Nevertheless, the figure unambiguously shows that tubes with diameters close to (5,5) grow most rapidly and the growth time increases with increasing diameter. For very small tubes, the growth time increases again.

Because the C_{60} fullerenes decay much faster than the inner tubes emerge, we looked for intermediate phases into which C_{60} might be transformed. The frequencies of the tangential modes decrease with decreasing tube diameter.[20] Thus, it is reasonable to expect the tangential phonon modes of such phases between the $A_g(2)$ mode of C_{60} and the G^+ mode of the outer tubes. Figure 6 shows this spectral region. Because of their low frequencies, the solid lines at 1504 and 1526 cm^{-1} in part (a) indicate the metallic A_1^{LO} (M) G mode components of the (7,4) and (8,2) and the (8,5) and (9,3) metallic inner tubes, respectively.[21] Because of the strongly nonlinear background, fitting the intensities of these lines is difficult. Nevertheless, one can safely say that the lower frequency mode emerges earlier than the higher one. Because

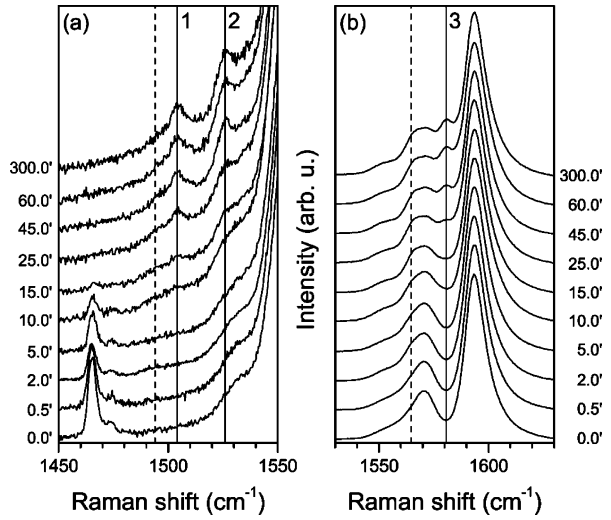

Figure 6. Spectral region of the tangential Raman modes measured with 488 nm in normal resolution at 80 K. Part (a) shows the LO G-mode components of the metallic tubes and part (b) shows the LO components of the semiconducting tubes. Solid lines indicate inner tube G mode components with the following assignment: 1, A_1^{LO} (M) of (7,4) and (8,2); 2, A_1^{LO} (M) of (8,5) and (9,3); and 3, A_1^{LO} (S) of (5,4) and (7,3). The dashed line in (a) indicates a spread-out response of a possible intermediate phase, while the dashed line in (b) indicates possible A_1^{TO} (M) components of small diameter metallic inner tubes.

the former is associated with smaller diameter tubes than the latter, this is in agreement with the RBM results. Around 1494 cm^{-1}, the lower A_1^{LO} (M) mode exhibits a broad shoulder (indicated by the dashed line), which after the 10 min transformation has about the same intensity as the 1504 cm^{-1} mode. However, after longer transformations, this mode does not increase any further. Thus, we conclude that this mode is not a G mode component but rather a fingerprint of an intermediate phase. In Figure 6b, the solid line at 1581 cm^{-1} indicates the A_1^{LO} (S) component of the (5,4) and (7,3) semiconducting inner tubes.[22,23] The dashed line at 1565 cm^{-1} can be assigned to the A_1^{TO} (M) components of the small diameter metallic inner tubes.

Additional information on the growth dynamics is obtained from the RBM cluster of a particular inner tube type. The most significant variation was found in the cluster of the (6,4) inner tubes, which can be studied with a 590 nm (2.10 eV) excitation. Figure 7 compares the high-resolution spectra of this cluster after the 2 and 300 min heat treatments. The spectra were scaled to equal intensity for the 346 cm^{-1} modes. Interestingly, in the small diameter outer tubes (diameter <1.34 nm), there is no indication for a dependence of the growth process of the (6,4) inner tube on the outer tube type. However, the relative volume fraction of the (6,4) tube in the large diameter outer tubes (diameter >1.34 nm) is larger after the 2 min than after the 300 min treatment. Thus, in the beginning, the (6,4) tubes grow faster in the larger tubes, but later on, the growth in the larger tubes is reduced although not completely inhibited. Additionally, there is practically no difference in the RBM linewidths between the 2 and 300 min transformed samples (the RBMs in the 676 nm spectra show also no change in line width).

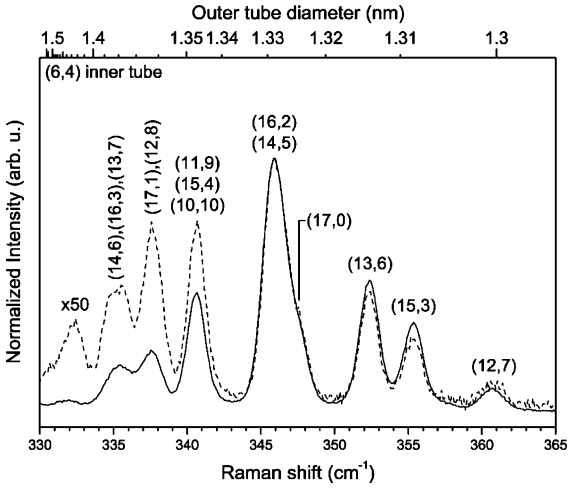

Figure 7. High-resolution Raman spectra of the (6,4) inner tube RBM cluster recorded with 590 nm at 80 K after 2 min (dashed) and 300 min (solid) annealing at 1250 °C. The different outer tubes in which the (6,4) inner tube was grown are indicated by their chiralities.[24] The top scale indicates the outer tube diameter.

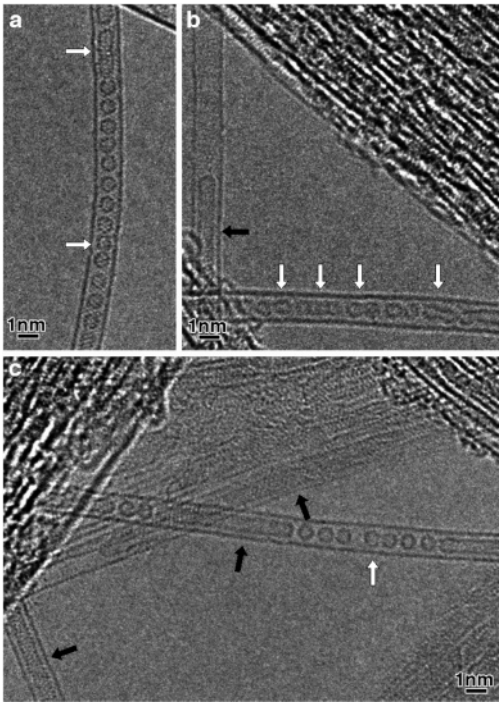

Figure 8. Selected HRTEM images of peapods transformed at 1250 °C after (a) 5 min, (b) 15 min, and (c) 25 min. The white and black arrows indicate modulated peapods (intermediate phase) and DWCNTs, respectively.

This indicates that the high perfection (long phonon lifetimes) of the inner tubes[3] is already established from the beginning of the growth.

Figure 8 shows three examples of HRTEM images of the peapods transformed at 1250 °C after 5, 15, and 25 min. After 5 min, there are only a few DWCNTs and still a considerable number of pristine C_{60}'s. However, coalescence has already started to a certain degree (white arrows), which removes the C_{60} units from resonance in Raman. After 15 min, the concentration of DWCNTs (black arrows) has clearly increased and, in addition, we see many fullerenes

in the process of coalescence (intermediate phase). All these tubes are out of resonance due to the shift in electronic structure. Thus, the Raman signal is fully lost but a quasiperiodic structure is retained. After 25 min, the DWCNTs dominate clearly even though there are still some fullerenes left. Most of them seem to be, however, already in the process of clustering together and therefore not observed in Raman.

The XRD data can be explained as follows: The small intensity of the (10) peak in the starting material indicates that a small amount of the SWCNTs is not filled. The sudden increase of this peak after starting the heating process is a consequence of expulsion of C_{60} molecules from a part of the filled tubes. It is very probable that in particular the large filled tubes are depleted, as the increase in the (10) peak is accompanied by a shift of the position of this peak to smaller q-values, i.e., larger tube diameters, both with the same half-time of 1.0(4) min. The observed delay of the loss of 1D chain periodicity is a fingerprint for initial reaction products with the same or almost the same periodicity as the fullerenes. The model calculation in Figure 2b starts with nearly 10% empty tubes and 90% filled tubes for the peapods before heat treatment. To match the experimental results, after 2 min exposure, the amount of empty tubes had to be increased to about 55% and was then kept constant at this value. The decrease of the (001) chain peak starts at about 5 min and is modeled by a decreasing amount of filled tubes, accompanied by a gradual increase of the amount of DWCNTs. After 45 min, this process is nearly completed resulting in 55% empty SWCNTs and 45% DWCNTs. For the long time annealing, a broad background at $q \approx 12$ nm^{-1} was added, which is possibly due to the emergence of some fractions of carbon, maybe amorphous, of the size of approximately 0.5 nm. A fine adjustment of the van der Waals radii improved the results: for the CNTs and for the fullerenes, the values were 0.325 and 0.31 nm, respectively. Both values are smaller than the lattice distance in single-crystal graphite of 0.336 nm. This means the introduction of the curvature of the carbon nanophase causes a decrease of the van der Waals distance.

The above results provide the following picture: When peapods (with mean diameters of 1.4 nm) are heated to temperatures around 1250 °C, within only 2 min, a noticeable fraction of fullerenes is expelled from the tubes, which causes the rapid decrease of the $A_g(2)$ Raman mode and the rapid increase of the (10) XRD peak. Since there is almost no intensity decrease of the (001) chain peak in the first 5 min, the fullerenes have to be depleted from the large diameter tubes, where they form a zigzag pattern instead of a 1D chain.[25,26] After about 2 min, no more fullerenes escape from the tubes and the remaining fullerenes are transformed into inner tubes.

The 1D chain peak is remarkably robust with respect to position and width and remains observable for a rather long time during transformation. Hence the periodicity within the tubes is retained even when the geometry and electronic structure of the fullerenes is already considerably modulated such that the Raman signal vanishes. This is consistent with the results of molecular dynamics simulations of the transformation process[27] and with the TEM analysis discussed below. Thus, a major decomposition of the fullerenes into smaller units (e.g., C_2) from which the inner tubes are built can be ruled out. This conclusion is backed up by a recent Raman and theoretical analysis using different ^{13}C enrichment levels of the fullerenes.[28] In that paper, the lack of any diffusion of the C atoms inside the SWCNTs during the inner tube growth process was demonstrated.

Because the C_{60} molecules decay much faster than the inner tubes grow, the majority of the latter cannot be formed by direct coalescence of pristine fullerenes. There needs to be some intermediate phase. This character of the coalescence process is clearly seen from the HRTEM results. After 5 min annealing, mostly pristine peapods dominate, but the transient phase is already seen. After 15 min, the transient phase dominates, although one can still find some peapods. Finally, most of the tubes are in a DWCNT phase after 25 min. Also, the shoulder to the emerging inner tube G modes at 1494 cm^{-1} is a fingerprint of an intermediate phase.

The formation times of the inner tubes depend strongly on the diameter. From the coalescence model,[29−31] one would expect that the first coalescence step is the formation of (5,5) tubes from which all other inner tube types are formed by further Stone−Wales bond rotations.[13] Thus, inner tubes with diameters close to that of the (5,5) tube should grow fastest as it was observed. For example, the (7,2) needs to shrink in diameter by about 5%, whereas the (8,3) needs to increase in diameter by about 13% (see Figure 5). In addition to diameter, the tube growth can be influenced by the formation of the tube caps.[32] In the case of fullerene coalescence, the caps are preformed for a (5,5) tube and have to be modified for other tube types. Especially for tubes with a smaller diameter than (5,5), the isolated pentagon rule for the caps can no longer be fulfilled.

The volume fraction of especially the (8,3) tube increases by a factor of almost 8.6 between the 15 and 60 min transformations. At these times, more than half of the 1D chain and definitely all pristine C_{60} were already destroyed. However, in the same time, the volume fractions of the (6,5) and (6,4) tubes increase by a factor of 4.5 and 2.7, respectively, and the intensity of the (7,2) increases only by a factor of 2.1. Considering additionally the growth curves in Figure 4, one can say that in the first phase mainly the small diameter inner tubes grow and in the second phase mainly the large diameter inner tubes grow. Although there are slight changes within the clusters of specific tubes, we could not observe that the whole cluster of a small diameter inner tube decreased while the cluster of a larger diameter inner tube increased. Thus we can rule out that small inner tubes are transformed into large inner tubes during the second growth phase.

The above discussion of the inner tube growth is in strong contrast to a recently identified growth process of inner tubes from ferrocene ($FeCp_2$) encapsulates. In this case, the inner tubes grow already at 600 °C within 1 h.[33] The RBM frequencies of C_{60} and $FeCp_2$ based inner tubes are identical, however, the intensity distribution and thus the volume

fractions of specific inner−outer tube pairs are different (even when the same SWCNTs starting material is used). In the case of $FeCp_2$, a direct coalescence of the precursor molecules into inner tubes can be ruled out. Rather, the presence of Fe inside the SWCNTs leads to a catalytic growth that is completely different from the growth from peapods.

In summary, we have studied the growth process of the inner tubes of C_{60} peapods based DWCNTs with Raman spectroscopy, XRD, and HRTEM. We showed that the C_{60} molecules decay almost a factor 5 faster than the 1D chain that is formed by these molecules. The small diameter inner tubes grow in about the same time in which the 1D chain decays, but the large diameter inner tubes grow about a factor 2 slower. The discrepancy between the time constant for the decay of the fullerenes and the growth of the inner tubes gives evidence for the existence of an intermediate phase. From the XRD data, this phase is solid and has basically the periodicity of the starting peapod system.

Acknowledgment. Valuable discussions with J. E. Fischer, D. Tománek, L. Forró, and M. Neumann are gratefully acknowledged. Work was financially supported by FWF projects P17345 and I83-N20 (ESF IMPRESS). Work on electron microscopy is partially supported by CREST. Hi.K. acknowledges KAKENHI, MEXT, Japan.

Supporting Information Available: Experimental methods. This material is available free of charge via the Internet at http://pubs.acs.org.

References

(1) Endo, M.; Muramatsu, H.; Hayashi, T.; Kim, Y. A.; Terrones, M.; Dresselhaus, M. S. *Nature* **2005**, *433*, 476.
(2) Bandow, S.; Takizawa, M.; Hirahara, K.; Yudasaka, M.; Iijima, S. *Chem. Phys. Lett.* **2001**, *337*, 48.
(3) Pfeiffer, R.; Kuzmany, H.; Kramberger, C.; Schaman, C.; Pichler, T.; Kataura, H.; Achiba, Y.; Kürti, J.; Zólyomi, V. *Phys. Rev. Lett.* **2003**, *90*, 225501.
(4) Simon, F.; Kramberger, C.; Pfeiffer, R.; Kuzmany, H.; Zólyomi, V.; Kürti, J.; Singer, P. M.; Alloul, H. *Phys. Rev. Lett.* **2005**, *95*, 017401.
(5) Singer, P. M.; Wzietek, P.; Alloul, H.; Simon, F.; Kuzmany, H. *Phys. Rev. Lett.* **2005**, *95*, 236403.
(6) Simon, F.; Kukovecz, Á.; Kramberger, C.; Pfeiffer, R.; Hasi, F.; Kuzmany, H.; Kataura, H. *Phys. Rev. B* **2005**, *71*, 165439.
(7) Kuzmany, H.; Plank, W.; Hulman, M.; Kramberger, C.; Grüneis, A.; Pichler, T.; Peterlik, H.; Kataura, H.; Achiba, Y. *Eur. Phys. J. B* **2001**, *22*, 307.
(8) Fantini, C.; Jorio, A.; Souza, M.; Strano, M. S.; Dresselhaus, M. S.; Pimenta, M. A. *Phys. Rev. Lett.* **2004**, *93*, 147406.
(9) Telg, H.; Maultzsch, J.; Reich, S.; Hennrich, F.; Thomsen, C. *Phys. Rev. Lett.* **2004**, *93*, 177401.
(10) Pfeiffer, R.; Simon, F.; Kuzmany, H.; Popov, V. N. *Phys. Rev. B* **2005**, *72*, 161404(R).
(11) Pfeiffer, R.; Kramberger, C.; Simon, F.; Kuzmany, H.; Popov, V. N.; Kataura, H. *Eur. Phys. J. B* **2004**, *42*, 345.
(12) Simon, F.; Kuzmany, H.; Rauf, H.; Pichler, T.; Bernardi, J.; Peterlik, H.; Korecz, L.; Fülöp, F.; Jánossy, A. *Chem. Phys. Lett.* **2004**, *383*, 362.
(13) Bandow, S.; Hiraoka, T.; Yumura, T.; Hirahara, K.; Shinohara, H.; Iijima, S. *Chem. Phys. Lett.* **2004**, *384*, 320.
(14) Kramberger, C.; Waske, A.; Biedermann, K.; Pichler, T.; Gemming, T.; Büchner, B.; Kataura, H. *Chem. Phys. Lett.* **2005**, *407*, 254.
(15) Abe, M.; Kataura, H.; Kira, H.; Kodama, T.; Suzuki, S.; Achiba, Y.; Kato, K.-i.; Takata, M.; Fujiwara, A.; Matsuda, K.; Maniwa, Y. *Phys. Rev. B* **2003**, *68*, 041405(R).
(16) Kataura, H.; Maniwa, Y.; Kodama, T.; Kikuchi, K.; Hirahara, K.; Suenaga, K.; Iijima, S.; Suzuki, S.; Achiba, Y.; Krätschmer, W. *Synth. Met.* **2001**, *121*, 1195.
(17) Pfeiffer, R.; Kuzmany, H.; Pichler, T.; Kataura, H.; Achiba, Y.; Melle-Franco, M.; Zerbetto, F. *Phys. Rev. B* **2004**, *69*, 035404.
(18) Cambedouzou, J.; Pichot, V.; Rols, S.; Launois, P.; Petit, P.; Klement, R.; Kataura, H.; Almairac, R. *Eur. Phys. J. B* **2004**, *42*, 31.
(19) Kramberger, C.; Pfeiffer, R.; Kuzmany, H.; Zólyomi, V.; Kürti, J. *Phys. Rev. B* **2003**, *68*, 235404.
(20) Dubay, O.; Kresse, G.; Kuzmany, H. *Phys. Rev. Lett.* **2002**, *88*, 235506.
(21) Piscanec, S.; Lazzeri, M.; Robertson, J.; Ferrari, A. C.; Mauri, F. *Phys. Rev. B* **2007**, *75*, 035427.
(22) Popov, V. N.; Lambin, P. *Phys. Rev. B* **2006**, *73*, 085407.
(23) Popov, V. N.; Lambin, P. *Phys. Rev. B* **2006**, *73*, 165425.
(24) Pfeiffer, R.; Simon, F.; Kuzmany, H.; Popov, V. N.; Zólyomi, V.; Kürti, J. *Phys. Status Solidi, B* **2006**, *243*, 3268.
(25) Michel, K. H.; Verberck, B.; Nikolaev, A. V. *Phys. Rev. Lett.* **2005**, *95*, 185506.
(26) Michel, K. H.; Verberck, B.; Nikolaev, A. V. *Eur. Phys. J.* **2005**, *48*, 113.
(27) Hernández, E.; Meunier, V.; Smith, B. W.; Rurali, R.; Terrones, H.; Buongiorno Nardelli, M.; Terrones, M.; Luzzi, D. E.; Charlier, J.-C. *Nano Lett.* **2003**, *3*, 1037.
(28) Zólyomi, V.; Simon, F.; Rusznyák, Á.; Pfeiffer, R.; Peterlik, H.; Kuzmany, H.; Kürti, J. *Phys. Rev. B* **2007**, *75*, 195419.
(29) Kim, Y.-H.; Lee, I.-H.; Chang, K. J.; Lee, S. *Phys. Rev. Lett.* **2003**, *90*, 065501.
(30) Zhao, Y.; Lin, Y.; Yakobson, B. I. *Phys. Rev. B* **2003**, *68*, 233403.
(31) Han, S.; Yoon, M.; Berber, S.; Park, N.; Osawa, E.; Ihm, J.; Tománek, D. *Phys. Rev. B* **2004**, *70*, 113402.
(32) Reich, S.; Li, L.; Robertson, J. *Phys. Rev. B* **2005**, *72*, 165423.
(33) Shiozawa, H.; Pichler, T.; Grüneis, A.; Pfeiffer, R.; Kuzmany, H.; Liu, Z.; Suenaga, K.; Kataura, H. *Adv. Mater.* submitted.

NL071107O